

Supporting Information

Zinc Chelation with Hydroxamate in Histone Deacetylases Modulated by Water Access to the Linker Binding Channel

Ruibo Wu^{1,2}, Zhenyu Lu,² Zexing Cao^{1} and Yingkai Zhang^{2*}.*

¹ Department of Chemistry and State Key Laboratory of Physical Chemistry of Solid Surfaces,
Xiamen University, Xiamen 361005, China E-mail: zxcao@xmu.edu.cn

² Department of Chemistry, New York University, New York, NY 10003 USA E-mail: Yingkai.zhang@nyu.edu

Computational details; The active site geometries of HDAC8, HDAC7 and HDAC4 enzyme-inhibitor complexes; Distributions of hydroxamate oxygen-zinc distances for each model from QM/MM MD simulations; The chelation mode and hydrogen bond network for HDAC4 (state B); The binding pockets (side-view and top-view) in selected models; Averaged ESP charge on the zinc ion in each model; The volume of active pocket in selected models; The complete list of references 16 and 37.

Computational details

Our simulation protocol is very similar to those employed in our previous studies of HDAC8^{1,2}.

1. Preparation of simulation systems

All HDAC8 models were built based on the crystal structure of 1T69,³ a HDAC8-SAHA complex. Firstly, the missing residues were added by the Swiss-PdbViewer.⁴ The mutant models were prepared with Swiss-PdbViewer⁴ based on the same crystal structure. We determined the protonation states of charged residues in the enzyme complex via H++ program⁵. His180 was determined as singly protonated on δ site, while His143 and His142 were determined as singly protonated on ϵ site. The same protocol has been employed to build HDAC7 and HDAC4 models base on crystal structures of 3COZ⁶ and 2VQM⁷ respectively. For HDAC4, considering that the five-member ring of the linker in the crystal structure⁷ is very different from SAHA and would pose some difficulties for QM/MM partition, we kept the initial length of linker but modified the 5-member ring in the linker (shown in Figure 1) to a SAHA-like straight-chain linker (shown in Figure S1). In this way, inhibitor linker components in our simulated three HDAC enzymes are quite similar.

Each prepared system was neutralized by adding Na⁺ ion at the protein surface with the Amber tool, and was solvated into a rectangular box with a 8-10 Å buffer distance between the solvent box wall and the nearest solute atoms. By employing AMBER10 molecular dynamics package⁸, it was first minimized and equilibrated, and then simulated for at least 3 ns with periodic boundary condition with a time step of 2 fs, temperature at 300 K and pressure at 1 atm. The trajectory was stable, and the resulted snapshot was employed for preparing subsequent QM/MM studies. The Amber99SB⁹⁻¹¹ force field for the protein and TIP3P model¹² for water molecules

were employed. We also utilized AMBER tools to generate atomic charges for SAHA or SAHA-like inhibitors and the rest of the parameters were from AMBER GAFF force field¹³. The Zn²⁺ ion was modeled with the Stote's scheme¹⁴, and 1500 kcal/mol/Å harmonic restraint was placed on ~15 atoms in the zinc binding site to retain the zinc coordination structure during the MM minimizations and dynamics simulations since zinc coordination shell is very difficult to be properly described by a molecular mechanical force field¹⁵⁻¹⁸

2. Born-Oppenheimer ab initio QM/MM MD simulations

With the snapshots taken from the classical MD trajectory, the QM/MM models were prepared by deleting the solvent molecules which are beyond 30 Å of the zinc atom in the active site. The His142, His143, Asp178, His180, Asp267, SAHA and zinc ion in HDAC8 models (similar choice for HDAC7/-4) were chosen as the QM subsystem with B3LYP functional and Stuttgart ECP/basis set¹⁹ (SDD) for the zinc atom and 6-31G(d) basis set for all other QM atoms. The QM/MM boundaries were described by the improved pseudobond approach²⁰⁻²³. All other atoms were described by the same molecular mechanical force field used in classical MD simulations. The spherical boundary condition was applied and the atoms 22 Å beyond from the zinc atom were fixed. The 18 and 12 Å cutoffs were employed for electrostatic and van der Waals interactions, respectively. There was no cutoff for electrostatic interactions between QM and MM regions. The prepared system was first minimized by QM/MM optimization. Then, 25 ps ab initio QM/MM MD simulations were carried out with the time step 1 fs and the Beeman algorithm²⁴ to integrate the Newton equations of motion, as well as the Berendsen thermostat method²⁵ to control the system temperature at 300 K. All ab initio QM/MM calculations were performed in modified Q-Chem²⁶ and Tinker²⁷ programs.

3. Determination of the free energy profile

To study the hydrogen transfer from SAHA to His142 in HDAC8, we employed the distance between His:N^ε and SAHA:H (on O1) as the reaction coordinate, and used an iterative minimization procedure with the reaction coordinate driving method²² to first map out the minimum energy path (MEP) associated with the reaction coordinate. For each determined structure along the reaction path, first the MM subsystem was further equilibrated with 500 ps molecular mechanical MD simulation. Then the resulting snapshot was used as the starting structure for ab initio QM/MM MD simulations with umbrella sampling. Each window was simulated for 25 ps. The configurations after 5 ps for each window were collected for data analysis. The probability distributions along the reaction coordinate were determined for each window and pieced together with the WHAM^{28, 29} to calculate the free energy profile along the reaction coordinate. This computational protocol has successfully been applied to study several enzymes as well as chemical reactions in aqueous solution³⁰⁻³⁷.

Reference

1. Wu, R.; Hu, P.; Wang, S.; Cao, Z.; Zhang, Y., *J. Chem. Theory Comput.* **2010**, *6*, 337-343.
2. Wu, R.; Wang, S.; Zhou, N.; Cao, Z.; Zhang, Y., *J Am Chem Soc* **2010**, *132*, 9471-9479.
3. Somoza, J. R.; Skene, R. J.; Katz, B. A.; Mol, C.; Ho, J. D.; Jennings, A. J.; Luong, C.; Arvai, A.; Buggy, J. J.; Chi, E.; Tang, J.; Sang, B. C.; Verner, E.; Wynands, R.; Leahy, E. M.; Dougan, D. R.; Snell, G.; Navre, M.; Knuth, M. W.; Swanson, R. V.; McRee, D. E.; Tari, L. W., *Structure* **2004**, *12* (7), 1325-1334.
4. Guex, N.; Peitsch, M. C., *Electrophoresis* **1997**, *18* (15), 2714-2723.
5. Gordon, J. C.; Myers, J. B.; Folta, T.; Shojia, V.; Heath, L. S.; Onufriev, A., *Nucleic Acids Res* **2005**, *33*, W368-W371.
6. Schuetz, A.; Min, J.; Allali-Hassani, A.; Schapira, M.; Shuen, M.; Loppnau, P.; Mazitschek, R.; Kwiatkowski, N. P.; Lewis, T. A.; Maglathin, R. L.; McLean, T. H.; Bochkarev, A.; Plotnikov, A. N.; Vedadi, M.; Arrowsmith, C. H., *J Biol Chem* **2008**, *283* (17), 11355-11363.
7. Bottomley, M. J.; Lo Surdo, P.; Di Giovine, P.; Cirillo, A.; Scarpelli, R.; Ferrigno, F.; Jones, P.; Neddermann, P.; De Francesco, R.; Steinkuhler, C.; Gallinari, P.; Carfi, A., *J Biol Chem* **2008**, *283* (39), 26694-26704.
8. Case, D. A.; Darden, T. A.; Cheatham, T. E.; Simmerling, C. L.; Wang, J.; Duke, R. E.; Luo, R.; Crowley, M.; Walker, R. C.; Zhang, W.; Merz, K. M.; Wang, B.; Hayik, S.; Roitberg, A.; Seabra, G.; Kolossvary, I.; Wong, K. F.; Paesani, F.; Vanicek, J.; Wu, X.; Brozell, S. R.; Steinkuhler, T.; Gohlke, H.; Yang, L.; Tan, C.; Mongan, J.; Hornak, V.; Cui, G.; Mathews, D. H.; Seetin, M. G.; Sagui, C.; Babin, V.; Kollman, P. A., *AMBER 10*, University of California: San Francisco, CA. 2008.
9. Cornell, W. D.; Cieplak, P.; Bayly, C. I.; Gould, I. R.; Merz, K. M.; Ferguson, D. M.; Spellmeyer, D. C.; Fox, T.; Caldwell, J. W.; Kollman, P. A., *J Am Chem Soc* **1995**, *117* (19), 5179-5197.
10. Wang, J. M.; Cieplak, P.; Kollman, P. A., *J Comput Chem* **2000**, *21* (12), 1049-1074.
11. Hornak, V.; Abel, R.; Okur, A.; Strockbine, B.; Roitberg, A.; Simmerling, C., *Proteins-Structure Function and Bioinformatics* **2006**, *65* (3), 712-725.
12. Jorgensen, W. L.; Chandrasekhar, J.; Madura, J. D.; Impey, R. W.; Klein, M. L., *J Chem Phys* **1983**, *79* (2), 926-935.
13. Wang, J. M.; Wolf, R. M.; Caldwell, J. W.; Kollman, P. A.; Case, D. A., *J Comput Chem* **2004**, *25* (9), 1157-1174.
14. Stote, R. H.; Karplus, M., *PROTEINS: Structure, Function, and Genetics* **1995**, *23*, 12-31.
15. Liang, J. Y.; Lipscomb, W. N., *P Natl Acad Sci USA* **1990**, *87* (10), 3675-3679.
16. Pang, Y. P., *Proteins* **2001**, *45* (3), 183-189.
17. Karjiban, R. A.; Rahman, M. B. A.; Basri, M.; Salleh, A. B.; Jacobs, D.; Wahab, H. A., *Protein Journal* **2009**, *28* (1), 14-23.
18. Yan, C. L.; Xiu, Z. L.; Li, X. H.; Li, S. M.; Hao, C.; Teng, H., *Proteins-Structure Function and Bioinformatics* **2008**, *73* (1), 134-149.
19. Dolg, M.; Wedig, U.; Stoll, H.; Preuss, H., *J Chem Phys* **1987**, *86* (2), 866-872.
20. Zhang, Y. K., *Theor Chem Acc* **2006**, *116* (1-3), 43-50.
21. Zhang, Y. K.; Lee, T. S.; Yang, W. T., *J Chem Phys* **1999**, *110* (1), 46-54.
22. Zhang, Y. K.; Liu, H. Y.; Yang, W. T., *J Chem Phys* **2000**, *112* (8), 3483-3492.
23. Zhang, Y. K., *J Chem Phys* **2005**, *122* (2), 024114.
24. Beeman, D., *J Comput Phys* **1976**, *20* (2), 130-139.
25. Berendsen, H. J. C.; Postma, J. P. M.; Vangunsteren, W. F.; Dinola, A.; Haak, J. R., *J Chem Phys* **1984**, *81* (8), 3684-3690.
26. Shao, Y.; Molnar, L. F.; Jung, Y.; Kussmann J., O. C., Brown S. T., Gilbert A. T., Slipchenko L. V., Levchenko S.

V., O'Neill D. P., DiStasio R. A., Lochan R. C., Wang T., Beran G. J., Besley N. A., Herbert J. M., Lin C. Y., Van Voorhis T., Chien S. H., Sodt A., Steele R. P., Rassolov V. A., Maslen P. E., Korambath P. P., Adamson R. D., Austin B., Baker J., Byrd E. F., Dachsel H., Doerksen R. J., Dreuw A., Dunietz B. D., Dutoi A. D., Furlani T. R., Gwaltney S. R., Heyden A., Hirata S., Hsu C. P., Kedziora G., Khalliulin R. Z., Klunzinger P., Lee A. M., Lee M. S., Liang W., Lotan I., Nair N., Peters B., Proynov E.I., Pieniazek P.A., Rhee Y.M., Ritchie J., Rosta E., Sherrill C.D., Simmonett A.C., Subotnik J.E., Woodcock H.L., Zhang W., Bell A.T., Chakraborty A. K., Chipman D. M., Keil F. J., Warshel A., Hehre W. J., Schaefer H. F., Kong J., Krylov A. I., Gill P. M., and Head-Gordon M., *Q-Chem*, version 3.0; Q-chem, Inc.: Pittsburgh, PA, 2006.

27. Ponder, J. W., *TINKER, Software Tools for Molecular Design*, Version 4.2; 2004.
28. Souaille, M.; Roux, B., *Comput Phys Commun* **2001**, *135* (1), 40-57.
29. Kumar, S.; Bouzida, D.; Swendsen, R. H.; Kollman, P. A.; Rosenberg, J. M., *J Comput Chem* **1992**, *13* (8), 1011-1021.
30. Wang, S. L.; Hu, P.; Zhang, Y. K., *J. Phys. Chem. B* **2007**, *111* (14), 3758-3764.
31. Hu, P.; Wang, S.; Zhang, Y., *J. Am. Chem. Soc.* **2008**, *130* (12), 3806-3813.
32. Hu, P.; Wang, S. L.; Zhang, Y. K., *J. Am. Chem. Soc.* **2008**, *130* (49), 16721-16728.
33. Lu, Z. Y.; Zhang, Y. K., *J. Chem. Theory Comput.* **2008**, *4* (8), 1237-1248.
34. Ke, Z. H.; Wang, S. L.; Xie, D. Q.; Zhang, Y. K., *J. Phys. Chem. B* **2009**, *113* (52), 16705-16710.
35. Ke, Z. H.; Zhou, Y. Z.; Hu, P.; Wang, S. L.; Xie, D. Q.; Zhang, Y. K., *J. Phys. Chem. B* **2009**, *113* (38), 12750-12758.
36. Zheng, H.; Wang, S. L.; Zhang, Y. K., *J. Comput. Chem.* **2009**, *30* (16), 2706-2711.
37. Wu, R. B.; Hu, P.; Wang, S. L.; Cao, Z. X.; Zhang, Y. K., *J. Chem. Theory Comput.* **2010**, *6* (1), 337-343.
38. Patey, G. N.; Valleau, J. P., *J Chem Phys* **1975**, *63* (6), 2334-2339.

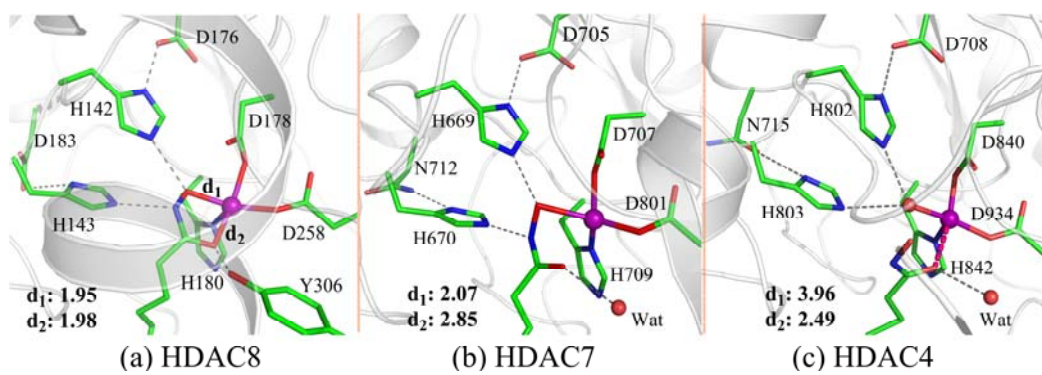


Figure S1. Illustration of active sites of initially prepared enzyme-inhibitor complexes for HDAC8, HDAC7 and HDAC4.

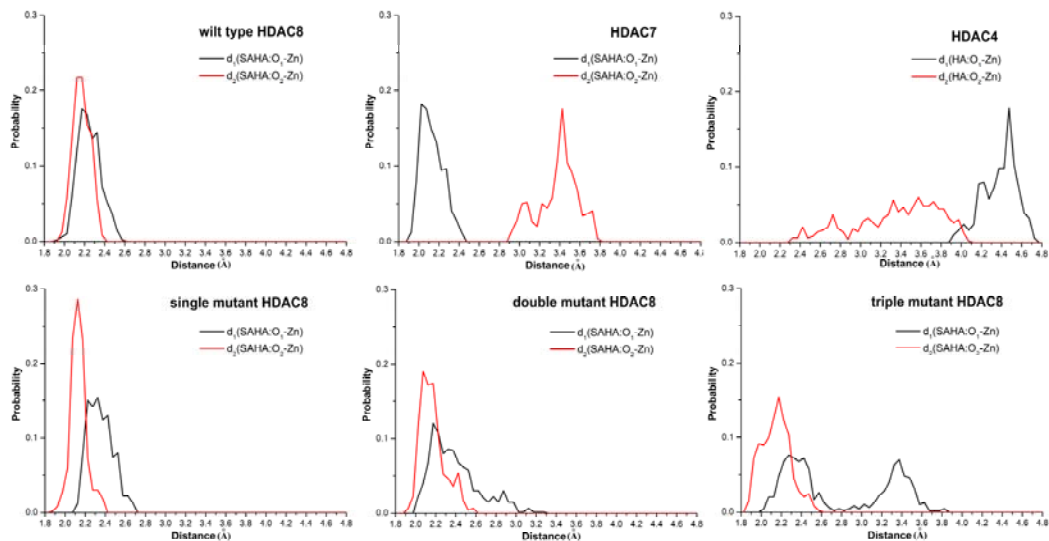


Figure S2. Distributions of hydroxamate oxygen-zinc distances (d_1 & d_2 in Figure 1a) from ab initio QM/MM MD simulations.

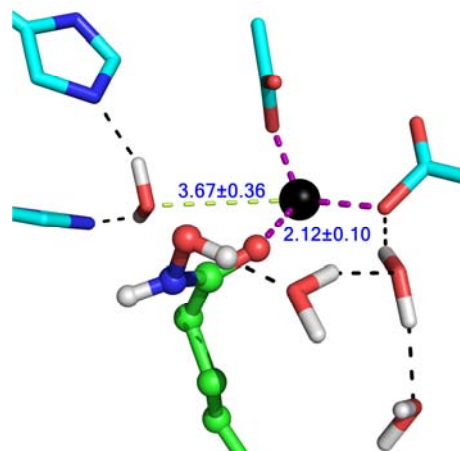


Figure S3. The chelation mode and hydrogen bond network for HDAC4 (state B).

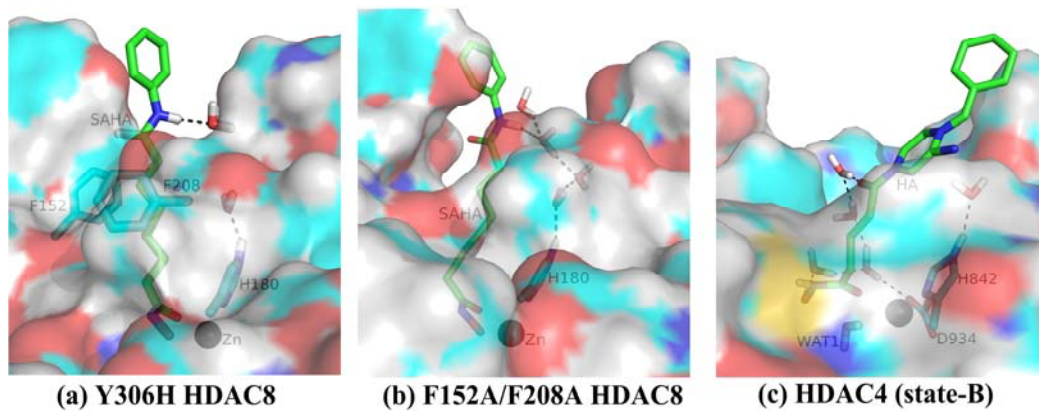


Figure S4. The binding pockets (sideview) in the selected models.

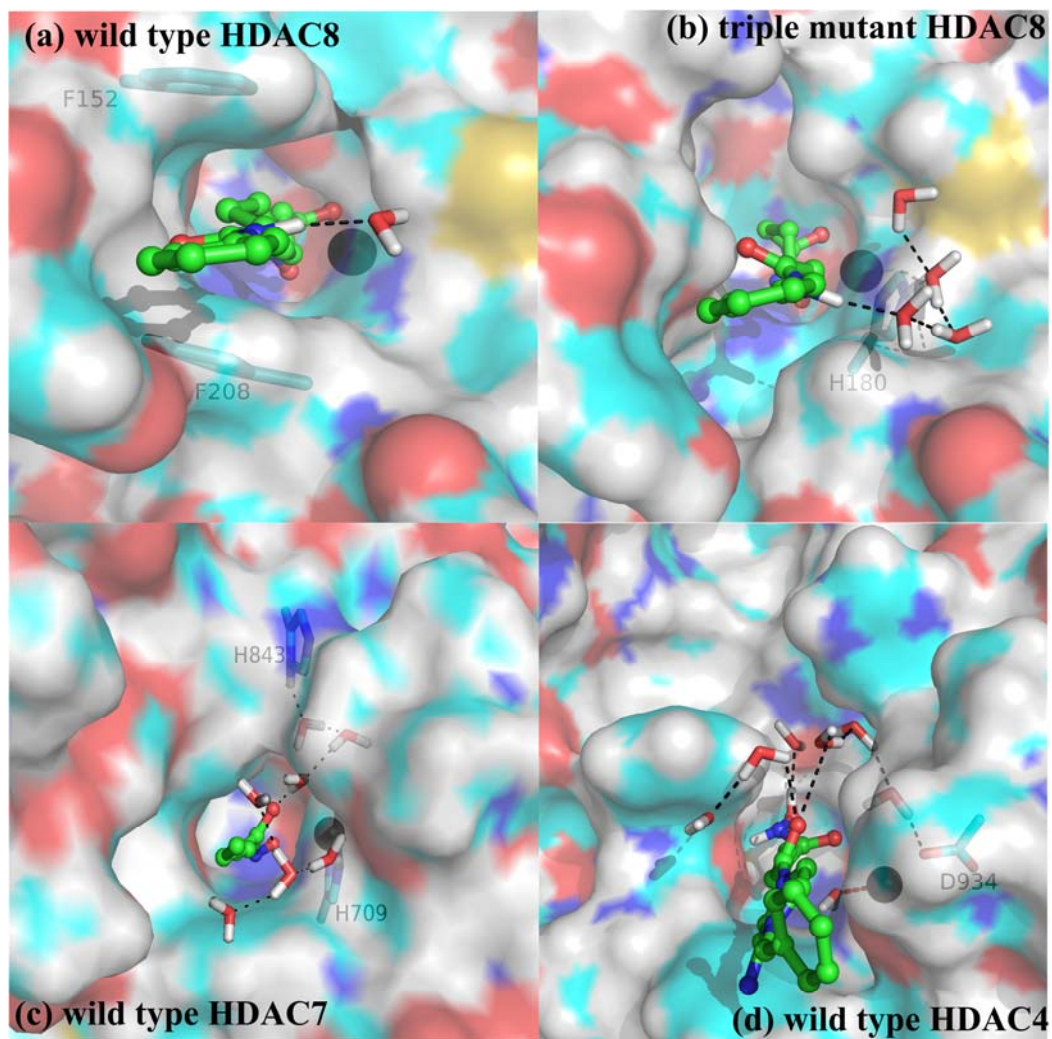


Figure S5. The surface and binding pocket (topview) of models shown in Figure 5.

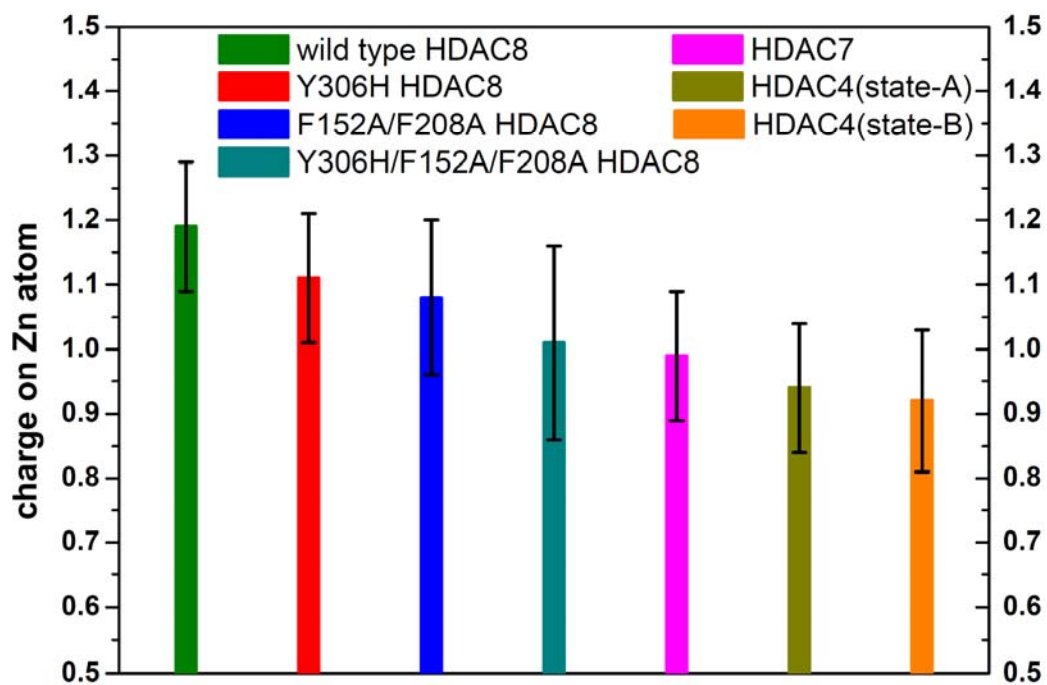


Figure S6. Averaged ESP charge of zinc in each model. The average values and error bars are calculated from the QM/MM MD snapshots.

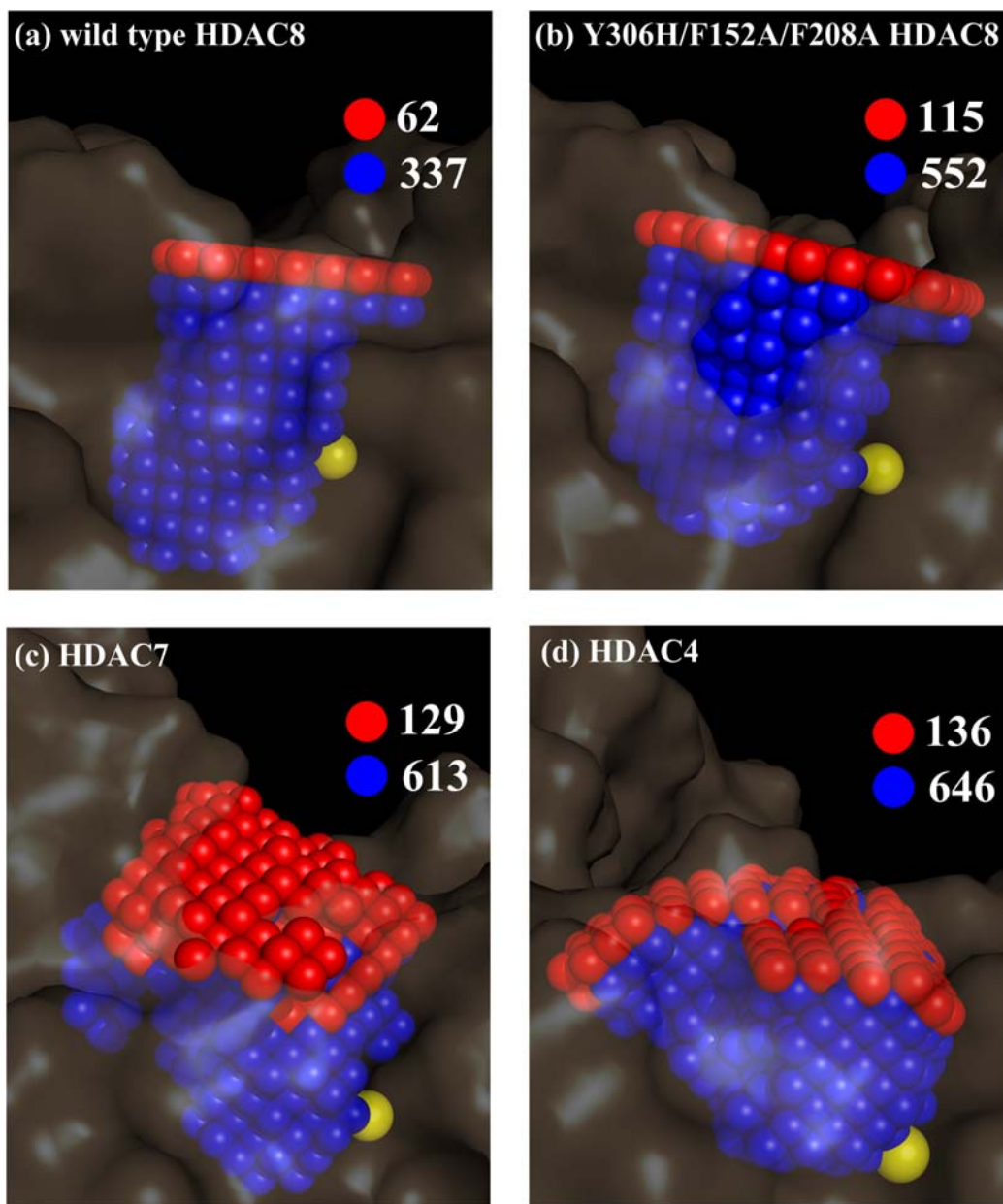


Figure S7. Volume of active pocket in the selected models. Calculation details: the cavity was occupied by dummy atoms (radius is 1.1 Å) using McMol program. The dummy atoms at the entrance of pocket is shown in red, and others shown in blue. Total numbers of dummy atoms are denoted in each figure. Taken model (a) as an example, the pocket volume is calculated as: $\frac{4}{3} * \Pi * (1.1 \text{ \AA})^3 * (62+337) = 2225 \text{ \AA}^3$.

Reference:

(16) Somoza, J. R.; Skene, R. J.; Katz, B. A.; Mol, C.; Ho, J. D.; Jennings, A. J.; Luong, C.; Arvai, A.; Buggy, J. J.; Chi, E.; Tang, J.; Sang, B. C.; Verner, E.; Wynands, R.; Leahy, E. M.; Dougan, D. R.; Snell, G.; Navre, M.; Knuth, M. W.; Swanson, R. V.; McRee, D. E.; Tari, L. W. *Structure* **2004**, *12*, 1325-1334.

(37) Shao, Y.; Molnar, L. F.; Jung, Y.; Kussmann J., O. C., Brown S. T., Gilbert A. T., Slipchenko L. V., Levchenko S. V., O'Neill D. P., DiStasio R. A., Lochan R. C., Wang T., Beran G. J., Besley N. A., Herbert J. M., Lin C. Y., Van Voorhis T., Chien S. H., Sodt A., Steele R. P., Rassolov V. A., Maslen P. E., Korambath P. P., Adamson R. D., Austin B., Baker J., Byrd E. F., Dachsel H., Doerksen R. J., Dreuw A., Dunietz B. D., Dutoi A. D., Furlani T. R., Gwaltney S. R., Heyden A., Hirata S., Hsu C. P., Kedziora G., Khalliulin R. Z., Klunzinger P., Lee A. M., Lee M. S., Liang W., Lotan I., Nair N., Peters B., Proynov E.I., Pieniazek P.A., Rhee Y.M., Ritchie J., Rosta E., Sherrill C.D., Simmonett A.C., Subotnik J.E., Woodcock H.L., Zhang W., Bell A.T., Chakraborty A. K., Chipman D. M., Keil F. J., Warshel A., Hehre W. J., Schaefer H. F., Kong J., Krylov A. I., Gill P. M., and Head-Gordon M. *Q-Chem*, version 3.0; Q-chem, Inc.: Pittsburgh, PA, 2006.